Exp Oncol 2022
44, 3, 217–221

Experimental ONCOLOGY

EFFECTS OF DEXTRAN-GRAFT-POLYACRYLAMIDE/ZnO NANOPARTICLES ON PROSTATE CANCER CELL LINES *IN VITRO*

*P.A. Virych[1, *], T.V. Zadvornyi[1], T.V. Borikun[1], O.O. Lykhova[1], V.A. Chumachenko[2], P.A. Virych[2], V.A. Pavlenko[2], N.V. Kutsevol[2], N.Yu. Lukianova[1]*

[1]R.E. Kavetsky Institute of Experimental Pathology, Oncology and Radiobiology, National Academy of Sciences of Ukraine, Kyiv 03022, Ukraine

[2]Taras Shevchenko National University of Kyiv, Kyiv 01033, Ukraine

***Background*: The combination of zinc oxide (ZnO) nanoparticles (NPs) with carriers enhances the anticancer effect of nanocomposites. *Aim:* To explore the mechanisms of cytotoxic action of dextran-graft-polyacrylamide (D-g-PAA/ZnO) NPs against prostate cancers cell lines *in vitro*. *Materials and Methods*: Dextran-polyacrylamide was used as a matrix for the synthesis of ZnO NPs. Prostate cancer cells LNCaP, DU-145 and PC-3 were treated with D-g-PAA/ZnO NPs. The expression of Bax, Bcl-2, p53 and Ki-67 was studied using immunocytochemical analysis. Cytomorphological changes in cells were detected after their incubation with nanocomposites for 24 h. *Results*: The treatment with D-g-PAA/ZnO NPs caused the increase in the Bax and p53 and the decrease in Ki-67 and Bcl-2 expression. Morphological changes associated with apoptosis were registered: decrease in cell size, appearance of cytoplasmic vacuolation, condensation of chromatin, blebbing. *Conclusions*: Treatment with D-g-PAA/ZnO nanocomposite led to the initiation of apoptotic cell death in prostate cancer cells *in vitro*.**

***Key Words:* apoptosis, nanoparticles, prostate cancer, zinc oxide.**

DOI: 10.32471/exp-oncology.2312-8852.vol-44-no-3.18452

Despite significant advances in medicine, cancer remains one of a major health threats worldwide. Conventional treatment approaches (chemotherapy, surgery, radiation therapy, etc) are not effective enough. Furthermore, chemotherapy causes severe side effects, and over time, cancer cells become resistant to anticancer agents. New approaches, such as targeted delivery of anticancer agents based on the nanosystems containing nanoparticles (NPs) and cytostatic drugs seem to be promising. This is facilitated by increased permeability of the tumor vascular network and impaired lymph circulation [1].

In recent years, nanotechnologies have shown a significant progress [2–3]. There have been developed NPs of metals and their oxides, liposomes, carbon nanotubes, polymer micelles and nanospheres etc [4] as well as zinc oxide (ZnO) NPs with unique physicochemical properties. ZnO NPs have high biocompatibility, which allows their use as an antibacterial, antifungal, antiviral and antitumor agents [5–6].

The antitumor effect of ZnO NPs is based on the ability of Zn^{2+} ions to regulate DNA replication, enzyme activity, cell proliferation and differentiation [7]. Interestingly, cancer cells lower the pH of tumor microenvironment, reducing effectiveness of chemotherapeutic agents. However, ZnO NPs in acidic environment dissociate, increasing the local concentration of Zn^{2+} [8]. Prostate tissues are characterized by a high zinc concentration that becomes significantly reduced during cancer development [9–10]. Based on these properties of prostate cancer cells, nanosystems with ZnO NPs can exert better permeability and provide the desired therapeutic effects.

Creation of delivery systems significantly improves the permeability of active ingredients and their accumulation in tumor cells. Polymer-based nanocarriers have a high biocompatibility, their structure is easily controlled and modified by functional groups. The 3D structure of polymers determines their capacity, and interaction with target cells due to the large number of functional groups relative to the system volume. The combination of ZnO NPs with carriers expands the potential antitumor properties of such nanocomposites [8, 11–15].

The aim of the study was to explore the mechanisms of cytotoxic action of dextran-graft-polyacrylamide (D-g-PAA)/ZnO NPs in prostate cancer cell lines *in vitro*.

MATERIALS AND METHODS

Cell lines. Prostate cancer cell lines of various malignancy degree (LNCaP, DU-145 and PC-3) were obtained from the Bank of Cell Lines from Human and Animal Tissues of the R.E. Kavetsky Institute of Experimental Pathology, Oncology and Radiobiology, National Academy of Sciences of Ukraine. Cells were incubated in DMEM medium with 4 mM L-glutamine (Biowest, France), 10% fetal calf serum (Biowest, France), 40 μg/ml gentamicin (Sigma, USA) at 37 °C and 5% CO_2 atmosphere.

Nanocomposites. The polymeric nanocarrier was synthesized by radical copolymerization as described in [16]. Star-like D-g-PAA copolymer possessed average number of polyacrylamide arms equal to 10, $M_n = 8.6 \cdot 10^5$ g/mol and polydispersity index Mw/Mn = 1.62. The synthesis of nanocomposite D-g-PAA/ZnO NPs was performed *in situ* in an aqueous solution of the biocompatible star-shaped copolymer dextran-

Submitted: September 5, 2022.
*Correspondence: E-mail: anabenasp@gmail.com
Abbreviations used: D-g-PAA – dextran-graft-polyacrylamide; FL – fluorescence; NPs – nanoparticles; ZnO — zinc oxide.

polyacrylamide (10 mg/ml) at room temperature from $ZnSO_4$ (0.1 M) with the addition of KOH (0.05 M).

The absorption spectra of nanocomposites were recorded with a Cary 60 UV-VIS spectrophotometer (Agilent, USA). The fluorescence (FL) spectra were recorded with a Shimadzu RF-6000 spectrofluorophotometer (Shimadzu, Japan) at the wavelength of 250 nm for FL excitation. The solution samples were placed in 1 × 1 × 4 cm polished quartz cell. The absorption and FL spectra were measured at room temperature.

Fig. 1 presents the absorption spectrum of ZnO NPs in D-g-PAA/ZnO NPs. It shows the clear exciton absorption peaks centered at 349 nm (3.5544 eV) for D-g-PAA/ZnO NPs. The exciton peaks were extracted from the total absorption spectra by peak-fitting of total spectra by basic Lorentz peak (Fig. 1, dotted line). This peak is blue shifted relative to corresponding peak in bulk ZnO (3.3 eV) by 0.2544 eV for D-g-PAA/ZnO NPs sample. Proceeding from above values of blue shift and taking the reference data on the size dependence of wavelength of exciton absorption peak for ZnO NPs, the size (diameter) of ZnO NPs in our sample was estimated as 3.6 nm for D-g-PAA/ZnO NPs [17].

Effects of D-g-PAA/ZnO NPs on cell growth. Cells were seeded ($1 \cdot 10^4$ cells/well) in 96-well plates (SPL, Korea) in DMEM medium (Biowest, France) with 10% FBS (Biowest, France) and 40 μg/ml gentamicin (Sigma, USA), and cultured for 24 h. Then, the D-g-PAA/ZnO NPs was added to cells in different concentration (ranging from 0.000781 to 0.05 M of ZnO NPs), and cells were further cultured for 24 h. The viability and proliferative activity of the cells was evaluated by staining the cells with crystal violet dye by the standard method (Sigma, USA) [18]. The results were registered at 540 nm using a spectrophotometer (Labsystems Multiskan PLUS, Finland). Number of the live cells in each well was routinely calculated. IC_{30} D-g-PAA/ZnO NPs concentrations were calculated by the method of regression analysis

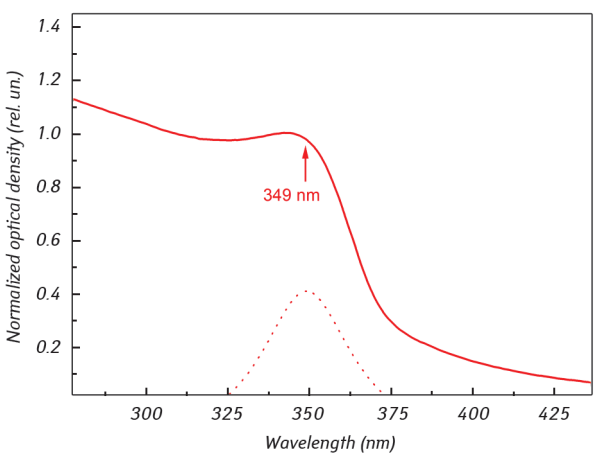

Fig. 1. Normalized absorption spectrum of D-g-PAA/ZnO NPs in aqueous solution. The dotted lines present the exciton absorption peak extracted from the total spectrum. The spectrum was measured at room temperature

Cell morphology. Cells were grown on cover glasses for 24 h and conventionally stained by Romanovsky — Gimza. Cytomorphological examination was performed using a Primo Star microscope (Carl Zeiss, Germany).

Determination of apoptosis by light microscopy. Cells were stained with acridine orange (Sigma, USA) diluted in a concentration of 12.5 mg/ml in a phosphate buffer (pH=6.4–6.5) *ex tempore*. Apoptotic cells (green nuclei, condensed chromatin) were counted (scored per 500 cells) [19].

Immunocytochemical methods. Cells were fixed in a cooled mixture of methanol: acetone 1:1 at –20 °C for 120 min and washed with phosphate buffer. Primary monoclonal antibodies anti-Ki-67 (clone SP6, Thermo Scientific, USA), anti-p53 (clone DO-7, Thermo Scientific, USA), anti-Bax (clone 6A7, Thermo Scientific, USA), anti-Bcl-2 (clone 100/D5, Thermo Scientific, USA) were used. Antibodies were diluted in blocking buffer. Cells were incubated with antibodies for 1 h. Ultra-Vision LP detection system (Thermo Scientific, USA) was used. After washing, the immunoprecipitation reaction was visualized using the DAB Quanto system (Thermo Scientific, USA). The color intensity was evaluated by the H-score method:

$$S = 0 \cdot N_0(\%) + 3 \cdot N_1(\%) + 2 \cdot N_2(\%) + 1 \cdot N_3(\%),$$

where S — H-score index, N_0 — cell number without staining, N_1, N_2, N_3 — cell number with low, medium or high levels of marker expression, respectively [20].

Comet assay. A standard method of alkaline gel electrophoresis of isolated cells was performed as described previously [21]. Microscopic analysis was performed using a fluorescent microscope AxioScope A.1 (Carl Zeiss, Germany). For each analyzed specimen, at least 100 "DNA-comets" were assessed. Digital images were analyzed by the computer program "CometScore" (TriTek Corp., USA).

Statistical analysis. Statistical processing was performed by Shapiro — Wilk tests ($p > 0.05$) and ANOVA Scheffe test ($p < 0.05$) with Origin v. 8.0 (OriginLab Corp., USA). The experiments were repeated in triplicate.

RESULTS AND DISCUSION

IC_{30} D-g-PAA/ZnO NPs concentrations for cell lines under study were estimated as follows: 2.76 mM for LNCaP cells, 2.48 mM for DU-145 cells and 1.96 mM for PC-3 cells. The following experiments were performed with D-g-PAA/ZnO NPs concentrations corresponding to IC_{30} for each cell line.

Morphological study of LNCaP, DU-145 and PC-3 cells indicated predominantly apoptotic pathway of cell death after D-g-PAA/ZnO NPs treatment (Fig. 2). Morphological changes typical of the initial stages of apoptosis were revealed: reduction of cell size, appearance of cytoplasmic vacuolation, chromatin aggregation in the nucleus. The number of cells at different mitosis stages decreased. The apoptosis induction was most pronounced in DU-145 cells (Fig. 2, *a*, *b*) approaching 26% of cells. Meanwhile,

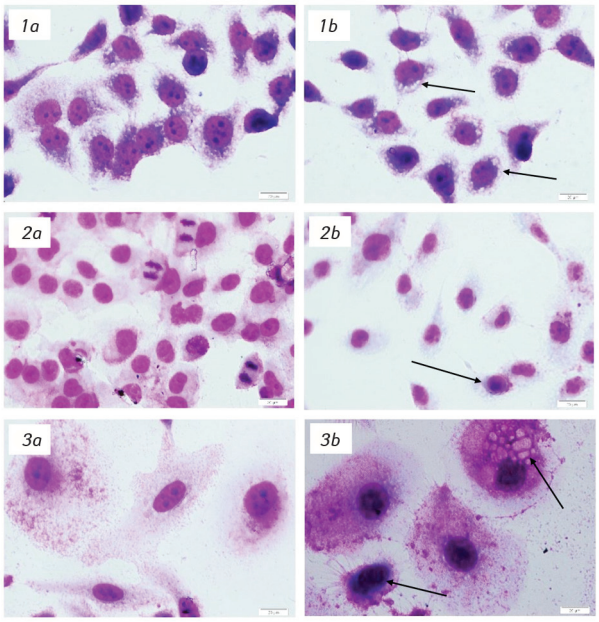

Fig. 2. Morphological changes of prostate cancer cell lines: LNCaP (*1*), DU-145 (*2*), PC-3 (*3*): *a* — control without treatment; *b* — after D-g-PAA/ZnO NPs treatment; stained by Romanovsky — Gimza; arrows point on cytoplasmic vacuolization and chromatin condensation in the nuclei

we did not detect changes in the morphology of nucleus and chromatin characteristic of necrosis (fade chromatin, nucleus shrink, etc). The typical apoptotic nuclei in the treated DU-145 cells stained with acridine orange were evident (Fig. 3). It should be noted that in control cultures of all cell lines under study, the number of cells in the state of apoptosis did not exceed 4%.

The effects of D-g-PAA/ZnO NPs at IC_{30} dose on prostate cancer cells were assessed also using "comet assay" (Table, Fig. 4). As can be seen from Table 1, LNCaP cells were less sensitive to the damaging effects of D-g-PAA/ZnO NPs compared to DU-145 and PC-3 cells.

Table. DNA content in the tail of "comet" in prostate cancer cells after treatment with D-g-PAA/ZnO NPs, %

Cell lines	DNA in tail, %	
	Control	D-g-PAA/ZnO NPs
LNCaP	7.15 ± 0.15	8.56 ± 2.93
DU-145	8.42 ± 0.55	15.54 ± 1.99*
PC-3	9.55 ± 0.48	16.41 ± 4.59*

Note: *The difference is significant compared to control, $p < 0.05$.

The expression of proapoptotic proteins Bax and p53 in LNCaP cells increased about twice after treatment with D-g-PAA/ZnO NPs. At the same time, the Ki-67 level in LNCaP cells was reduced by 3 times and Bcl-2 by 5 times. (Fig. 5, *a*). We detected similar changes in DU-145 cells characterized by highly malignant phenotype. The expression of the proapoptotic Bax protein remained unchanged, the expression of Ki-67 was reduced by 1.8 times, Bcl-2 — by 2.5 times and p53 expression increased by 2.3 times (Fig. 5, *b*). D-g-PAA/ZnO NPs treatment of PC-3 cells caused an increase of the expression of Bax and p53 proteins by 4 and 5 times, respectively, and 3-fold decrease of Ki-67 (Fig. 5, *c*). Therefore, D-g-PAA/ZnO NPs treatment initiated apoptotic cascade in prostate cancer cells.

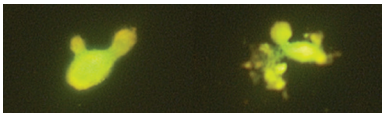

Fig. 3. Apoptotic changes in nuclei of DU-145 cells treated with D-g-PAA/ZnO NPs, ×400, acridine orange staining. Studied substance causes apoptotic death of prostate cancer cells, which have visible apoptotic bodies as well as membrane blebbing and protrusions

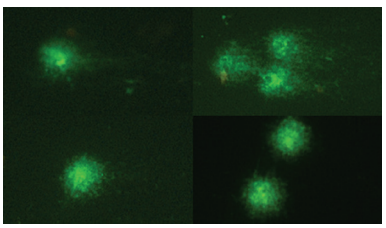

Fig. 4. Typical image of "comets" obtained by alkaline single-cell gel electrophoresis assay, ×400, acridine orange staining

Obtained data allow us to conclude that ZnO NPs exert cytotoxic activity in cultured prostate cancer cells via inducing apoptosis. Similar effects of ZnO NPs on p53, Bcl-2 and Bax expression were detected by other authors on a variety of cancer cell lines including liver cancer Huh7 cells [22], breast cancer MCF-7 and MDA-MB-231 cells [23, 24], melanoma cells [25], and colorectal cancer cells [26].

The data on the toxicity of zinc NPs vary. Sherzad *et al.* [27] found that DNA damage depends not only on the studied NPs but also on the target cell types. Zinc NPs exert significant cyto- and genotoxic effects on the cells of the human nasal mucosa [28], but not on neurons [29]. Kwon *et al.* [30] showed an absence of genotoxic effects in several *in vitro* and *in vivo* assays using particles of different sizes and charges. Without a doubt, the coating and composition of carriers could also affect the genotoxic potential of ZnO NPs.

The development of biotechnological methods for designing novel nanocomposites is important for meeting the needs of modern oncology. Due to their properties, NPs based on metal compounds are able to perform intercellular and intracellular transport of drugs, the controlled release of substances, and delivery of drug to the biotarget [31]. Among other NPs, ZnO NPs are the least studied. In experiments on isolated cells, it has been shown that these NPs are able to cause DNA damage directly or indirectly, contributing to the development of oxidative stress and inflammatory response [32]. They can penetrate cell membranes and directly interact with DNA in the nucleus. The use of ZnO NPs could be the most promising in the case of prostate cancer, as it is known that the development of malignant neoplasms is accompanied by a significant decrease in Zn level in prostate cells [33]. In the available literature, there is no consensus on the mechanism of action of zinc NPs on malignantly transformed cells. It is believed that the cytotoxic activity of zinc NPs depends on the method of their production and size as well as on the type

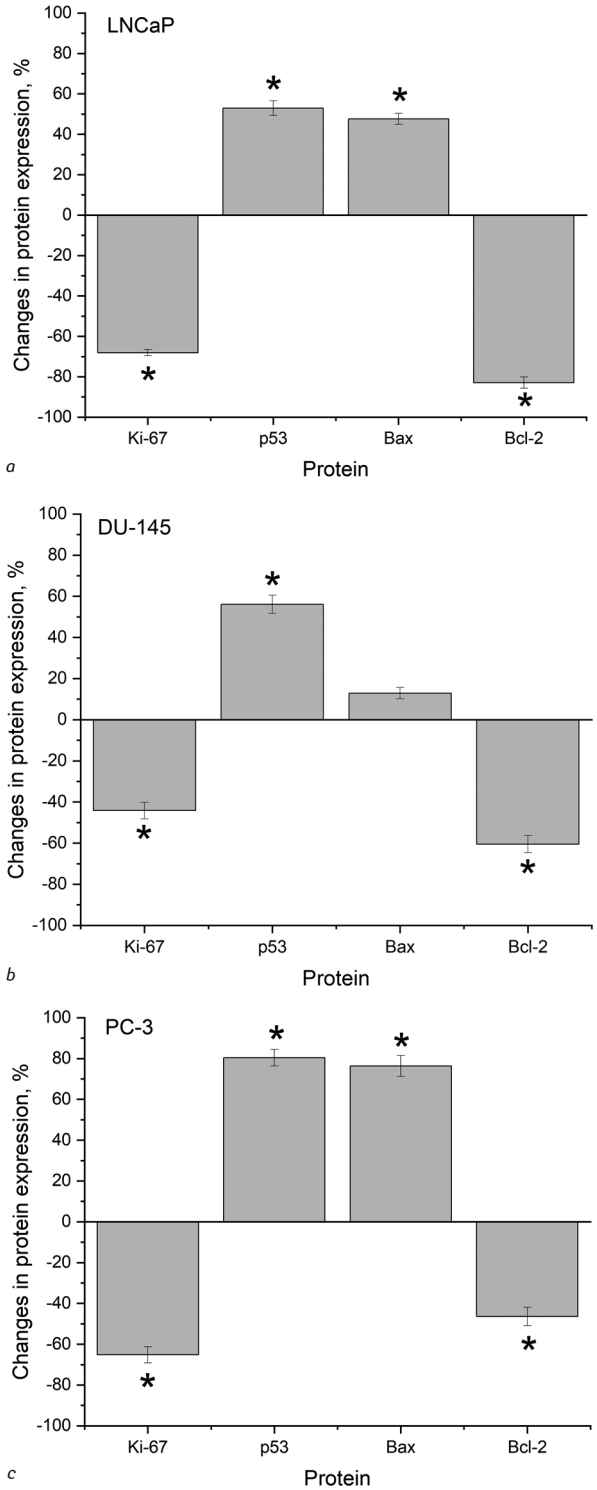

Fig. 5. Analysis of prostate cancer cells immunostaining for Ki-67, Bcl-2, Bax and p53 after D-g-PAA/ZnO NPs treatment: *a* — LNCaP cells; *b* — DU-154 cells; *c* — PC-3 cells. The change in H-score following culture in the presence of D-g-PAA/ZnO NPs is calculated as percentage. "0" line corresponds to protein expression in control cells. *The difference is significant compared to control, $p < 0.05$

of substances used as stabilizers. We have demonstrated that D-g-PAA/ZnO NPs induce apoptotic death of human prostate cancer cells of different malignancy degree. The most significant signs of apoptotic death as well as at the changes in the ratio of apoptosis regulatory proteins were recorded in the DU-145 cells. The obtained data undoubtedly point to the prospects of further exploration of the effects of D-g-PAA/ZnO NPs as well as other nanocomposites as the carriers of anticancer drugs.

ACKNOWLEDGMENTS

This work was funded by the research program of the NAS of Ukraine "The Role of Bone Remodeling Markers in the Formation of Malignancy Degree of the Most Common Hormone-Dependent Tumors" (0118U005468) and scientific grants of National Research Foundation of Ukraine Project (No. 2020.02/0022), Ministry of Education and Science of Ukraine Project (N0122U001818; 22BP037012).

REFERENCES

1. **Rahim MA, Jan N, Khan S, *et al.*** Recent advancements in stimuli responsive drug delivery platforms for active and passive cancer targeting. Cancers (Basel) 2021; **13**: 670. doi: 10.3390/cancers13040670

2. **Xu JJ, Zhang WC, Guo YW, *et al.*** Metal nanoparticles as a promising technology in targeted cancer treatment. Drug Deliv 2022; **29**: 664–78. doi: 10.1080/10717544.2022.2039804

3. **Li S, Zhang H, Chen K, *et al.*** Application of chitosan/alginate nanoparticle in oral drug delivery systems: prospects and challenges. Drug Deliv 2022; **29**: 1142–9. doi: 10.1080/10717544.2022.2058646

4. **Anjum S, Hashim M, Malik SA, *et al.*** Recent advances in zinc oxide nanoparticles (ZnO NPs) for cancer diagnosis, target drug delivery, and treatment. Cancers (Basel) 2021; **13**: 4570. doi: 10.3390/cancers13184570

5. **Wiesmann N, Tremel W, Brieger J.** Zinc oxide nanoparticles for therapeutic purposes in cancer medicine. J Mater Chem B 2020; **8**: 4973–89. doi: 10.1039/d0tb00739k

6. **Islam F, Shohag S, Uddin MJ, *et al.*** Exploring the journey of zinc oxide nanoparticles (ZnO-NPs) toward biomedical applications. Materials (Basel) 2022; **15**: 2160. doi: 10.3390/ma15062160

7. **Skrajnowska D, Bobrowska-Korczak B.** Role of zinc in immune system and anti-cancer defense mechanisms. Nutrients 2019; **11**: 2273. doi: 10.3390/nu11102273

8. **Singh TA, Das J, Sil PC.** Zinc oxide nanoparticles: A comprehensive review on its synthesis, anticancer and drug delivery applications as well as health risks. Adv Colloid Interface Sci 2020; **286**: 102317. doi: 10.1016/j.cis.2020.102317

9. **Li D, Stovall DB, Wang W, *et al.*** Advances of zinc signaling studies in prostate cancer. Int J Mol Sci 2020; **21**: 667. doi: 10.3390/ijms21020667

10. **Prasad RR, Raina K, Mishra N, *et al.*** Stage-specific differential expression of zinc transporter SLC30A and SLC39A family proteins during prostate tumorigenesis. Mol Carcinog 2022; **61**: 454–71. doi: 10.1002/mc.23382

11. **Hu C, Du W.** Zinc oxide nanoparticles (ZnO NPs) combined with cisplatin and gemcitabine inhibits tumor activity of NSCLC cells. Aging (Albany, NY) 2020; **12**: 25767–77. doi: 10.18632/aging.104187

12. **Wang Y, Zhang Y, Guo Y, *et al.*** Synthesis of Zinc oxide nanoparticles from Marsdenia tenacissima inhibits the cell proliferation and induces apoptosis in laryngeal cancer cells (Hep-2). J Photochem Photobiol B 2019; **201**: 111624. doi: 10.1016/j.jphotobiol.2019.111624

13. **Ruenraroengsak P, Kiryushko D, Theodorou IG, *et al.*** Frizzled-7-targeted delivery of zinc oxide nanoparticles to drug-resistant breast cancer cells. Nanoscale 2019; **11**: 12858–70. doi: 10.1039/c9nr01277j

14. **Liu J, Ma X, Jin S, *et al*.** Zinc oxide nanoparticles as adjuvant to facilitate doxorubicin intracellular accumulation and visualize pH-responsive release for overcoming drug resistance. Mol Pharm 2016; **13**: 1723–30. doi: 10.1021/acs.molpharmaceut.6b00311

15. **Wang J, Lee JS, Kim D, *et al*.** Exploration of zinc oxide nanoparticles as a multitarget and multifunctional anticancer nanomedicine. ACS Appl Mater Interfaces 2017; **9**: 39971–84. doi: 10.1021/acsami.7b11219

16. **Chernykh M, Zavalny D, Sokolova V, *et al*.** New water-soluble thermosensitive star-like copolymer as a promising carrier of the chemotherapeutic drug doxorubicin. Materials (Basel) 2021; **14**: 3517. doi: 10.3390/ma14133517

17. **Viswanatha R, Sapra S, Satpati B, *et al*.** Understanding the quantum size effects in ZnO nanocrystals. J Mat Chem 2004; **14**: 661–8. doi: 10.1039/B310404D

18. **Vega-Avila E, Pugsley MK**. An overview of colorimetric assay methods used to assess survival or proliferation of mammalian cells. Proc West Pharmacol Soc 2011; **54**: 10-4.

19. **Squier MK, Cohen JJ.** Standard quantitative assays for apoptosis. Mol Biotech 2001; **19**: 305–12. doi: 10.1385/MB:19:3:305

20. **McClelland RA, Wilson D, Leake R, *et al*.** A multicentre study into the reliability of steroid receptor immunocytochemical assay quantification. British Quality Control Group. Eur J Cancer 1991; **27**: 711–5. doi: 10.1016/0277-5379(91)90171-9

21. **Zadvornyi TV, Lukianova NY, Borikun TV, *et al***. Effects of exogenous lactoferrin on phenotypic profile and invasiveness of human prostate cancer cells (DU145 and LNCaP) *in vitro*. Exp Oncol 2018; 40: 184–9. doi: 10.31768/2312-8852.2018.40(3):184-189

22. **Yang R, Wu R, Mei J, *et al*.** Zinc oxide nanoparticles promotes liver cancer cell apoptosis through inducing autophagy and promoting p53. Eur Rev Med Pharmacol Sci 2021; **25**: 1557–63. doi: 10.26355/eurrev_202102_24864

23. **Khorsandi L, Farasat M.** Zinc oxide nanoparticles enhance expression of maspin in human breast cancer cells. Environ Sci Pollut Res Int 2020; **27**: 38300–10. doi: 10.1007/s11356-020-09986-5

24. **Pouresmaeil V, Haghighi S, Raeisalsadati AS, *et al*.** The anti-breast cancer effects of green-synthesized zinc oxide nanoparticles using carob extracts. Anticancer Agents Med Chem 2021; **21**: 316–26. doi: 10.2174/1871520620666200721132522

25. **Duan X, Liao Y, Liu T, *et al*.** Zinc oxide nanoparticles synthesized from Cardiospermum halicacabum and its anticancer activity in human melanoma cells (A375) through the modulation of apoptosis pathway. J Photochem Photobiol B. 2020; **202**: 111718. doi: 10.1016/j.jphotobiol.2019.1117185

26. **Berehu HM, S A, Khan MI, *et al*.** Cytotoxic potential of biogenic zinc oxide nanoparticles synthesized from *Swertia chirayita* leaf extract on colorectal cancer cells. Front Bioeng Biotechnol 2021; **9**: 788527. doi: 10.3389/fbioe.2021.788527

27. **Scherzad A, Meyer T, Kleinsasser N, *et al*.** Molecular mechanisms of zinc oxide nanoparticle-induced genotoxicity short. Materials (Basel) 2017; **10**: 1427. doi: 10.3390/ma10121427

28. **Hackenberg S, Scherzed A, Technau A, *et al*.** Cytotoxic, genotoxic and proinflammatory effects of zinc oxide nanoparticles in human nasal mucosa cells in vitro. Toxicol In Vitro 2011; **25**: 657–63. doi: 10.1016/j.tiv.2011.01.003

29. **Valdiglesias V, Costa C, Kilic G, *et al*.** Neuronal cytotoxicity and genotoxicity induced by zinc oxide nanoparticles. Environ Int 2013; **55**: 92–100. doi: 10.1016/j.envint.2013.02.013

30. **Kwon JY, Lee SY, Koedrith P, *et al*.** Lack of genotoxic potential of ZnO nanoparticles in in vitro and in vivo tests. Mutat Res Genet Toxicol Environ Mutagen 2014; **761**: 1–9. doi: 10.1016/j.mrgentox.2014.01.005

31. **Mundekkad D**, **Cho W.** Nanoparticles in clinical translation for cancer therapy. Int J Mol Sci 2022; **23**: 1685. doi: 10.3390/ijms23031685

32. **Bisht G, Rayamajhi S.** ZnO nanoparticles: a promising anticancer agent. Nanobiomedicine (Rij) 2016; **3**: 9. doi: 10.5772/63437

33. **Sauer AK, Vela H, Vela G, *et al*.** Zinc deficiency in men over 50 and its implications in prostate disorders. Front Oncol 2020; **10**: 1293. https://doi.org/10.3389/fonc.2020.01293

ПРОТИПУХЛИННА АКТИВНІСТЬ НАНОЧАСТИНОК ДЕКСТРАН-ПОЛІАКРИЛАМІДУ/ZnO ЩОДО ЛІНІЙ КЛІТИН РАКУ ПЕРЕДМІХУРОВОЇ ЗАЛОЗИ *IN VITRO*

П.А. Вірич[1], Т.В. Задворний[1], Т.В. Борікун[1], О.О. Лихова[1], В.А. Чумаченко[2], П.А. Вірич[2], В.А. Павленко[2], Н.В. Куцевол[2], Н.Ю. Лук'янова[1]

[1]Інститут експериментальної патології, онкології і радіобіології ім. Р.Є. Кавецького НАН України, Київ 03022, Україна

[2]Київський національний університет імені Тараса Шевченка, Київ 01033, Україна

Стан питання: Поєднання наночастинок (НЧ) оксиду цинку (ZnO) з носіями розширює потенційні властивості нанокомпозитів проти пухлин різного ступеня агресивності та стійкості до хіміопрепаратів. ***Мета:*** З'ясувати цитотоксичні механізми наносистем декстран-поліакриламіду (Д-ПАА)/ZnO в клітинних лініях раку передміхурової залози *in vitro*. ***Матеріали і методи:*** Д-ПАА було використано як матрицю для синтезу НЧ ZnO. Дослідження проводили *in vitro* на клітинних лініях раку передміхурової залози різного ступеня злоякісності LNCaP, DU-145 та PC-3. Рівні експресії Bax, Bcl-2, p53 і Ki-67 досліджували імуноцитохімічним методом. Цитоморфологічні зміни клітин виявляли після їх інкубації з нанокомпозитами протягом 24 год. ***Результати:*** Встановлено підвищення експресії проапоптотичних білків Bax і p53 не менше ніж у 2 рази для всіх ліній клітин після культивування з НЧ Д-ПАА/ZnO. Виявлено морфологічні зміни, пов'язані з апоптозом: зменшення розмірів клітин, поява цитоплазматичної вакуолізації, конденсація хроматину в ядрі, блеббінг. ***Висновки:*** Нанокомпозит Д-ПАА/ZnO НЧ впливає на експресію Bax, Bcl-2, p53 і Ki-67 у клітинних лініях раку передміхурової залози різного ступеня злоякісності *in vitro*, ініціюючи апоптотичну загибель клітин. Отримані результати свідчать про можливість використання цієї наносистеми для лікування пацієнтів з раком передміхурової залози.

Ключові слова: апоптоз, наночастинки, оксид цинку, рак передміхурової залози.